Modal analysis of sailplane and transport aircraft wings using the dynamic stiffness method

J R Banerjee

School of Mathematics, Computer Science and Engineering City University London, Northampton Square, London EC1V 0HB, UK

Abstract. The purpose of this paper is to provide theory, results, discussion and conclusions arising from an in-depth investigation on the modal behaviour of high aspect ratio aircraft wings. The illustrative examples chosen are representative of sailplane and transport airliner wings. To achieve this objective, the dynamic stiffness method of modal analysis is used. The wing is represented by a series of dynamic stiffness elements of bending-torsion coupled beams which are assembled to form the overall dynamic stiffness matrix of the complete wing. With cantilever boundary condition applied at the root, the eigenvalue problem is formulated and finally solved with the help of the Wittrick-Williams algorithm to yield the eigenvalues and eigenmodes which are essentially the natural frequencies and mode shapes of the wing. Results for wings of two sailplanes and four transport aircraft are discussed and finally some conclusions are drawn.

1. Introduction

Sailplane and transport aircraft wings are slender and flexible because of their high aspect ratios resulting from large spans and relatively short chords. As a consequence, they are easily prone to vibration problems. In this respect, modal analysis of aircraft wings, particularly those with high aspect ratios is very important. Sailplane and transport airliner wings are typical examples for which the investigation is of great significance. Indeed modal analysis plays an important role in the design of aircraft wings. An analysis of this kind is an obligatory airworthiness requirement which is rigorously enforced by the civil aviation authorities. The purpose of this paper is to carry out such an analysis and investigate the modal behaviour of sailplane and transport aircraft wings by applying the dynamic stiffness method.

   One of the main motivations for modal analysis of aircraft wings originates from that fact that it is a fundamental prerequisite to carry out an aeroelastic or response analysis, particularly when using the normal mode method. There are some published papers in this and related areas [1-7]. In general, the finite element method (FEM) is widely used to investigate the modal behaviour of aircraft wings. The FEM is an approximate method where the stiffness and mass properties of all individual elements are assembled to form the overall stiffness matrix **[K]** and mass matrix **[M]** of the structure which is an aircraft wing here. Then for modal analysis, upon imposing the boundary conditions, the typical eigenvalue problem of the type $[[K] - \lambda[M]]\{\Delta\} = 0$ is solved where $\{\Delta\}$ is the nodal displacement vector and the square root of λ gives the natural frequencies of the structure. The corresponding mode shapes are recovered in the usual way. In the FEM it is generally true that by increasing the number of elements in the analysis, the results become more and more accurate. It is acknowledged that the FEM is numerically intensive and the degrees of freedom identified by the order of **[K]** and **[M]** matrices decide the number of eigenvalues (which are essentially the natural frequencies) that can be computed.

The higher order natural frequencies will of course, be considerably less accurate. Against this background, there is an elegant and powerful alternative to the FEM for modal analysis of aircraft wings or any other structures. This method is the so-called dynamic stiffness method (DSM). The DSM unlike the FEM, relies on an exact single frequency dependent dynamic stiffness element containing both the mass and stiffness properties of the element as the basic building block. The assembly procedure in the DSM is essentially the same as it is in the FEM, but a single dynamic stiffness element matrix is used for each structural component instead of separate mass and stiffness matrices to form the overall frequency-dependent dynamic stiffness matrix **[K$_D$]** of the complete structure (wing). The eigenvalue problem is formulated as **[K$_D$]{Δ}**=0 where **{Δ}** is the nodal displacement vector comprising the amplitudes of nodal displacements. The next step is to extract the eigenvalues of the structure. At this point a significant difference with the FEM arises with regard to the solution technique. The formulation **[K$_D$]{Δ}**=0 leads to a transcendental (nonlinear) eigenvalue problem as opposed to the linear eigenvalue problem generally encountered in the FEM. The best available solution technique to extract the eigenvalues in the DSM is to apply the algorithm of Wittrick and Williams [8], known as the Wittrick-Williams algorithm in the literature which has featured in literally hundreds of papers. The algorithm which monitors the Sturm sequence property of the dynamic stiffness matrix is robust and it ensures that no natural frequency of the structure is missed.

   Within the above context, a range of aircraft wings is investigated for their free vibration characteristics in this paper. Two different categories of aircraft wings are analysed. They are essentially for sailplane and transport airliner wings. Two illustrative examples for the former and four for the latter are demonstrated when presenting numerical results. The investigation required considerable efforts for data preparation to model each of the wings. The dynamic stiffness method which provides the best possible model accuracy is used as mentioned. In idealising the wing, an assembly of the frequency dependent dynamic stiffness elements of bending-torsion coupled beams [9-10], comprising both the mass and stiffness properties is efficiently utilised. Natural frequencies and mode shapes computed from the dynamic stiffness method are compared and contrasted and finally some conclusions are drawn.

2. Theory

2.1 Dynamic stiffness matrix of a bending-torsion coupled beam
An aircraft wing such as the one shown in figure 1 is a classic example of a bending-torsion coupled beam. Such a representation is particularly relevant to analyse a high aspect ratio wing.
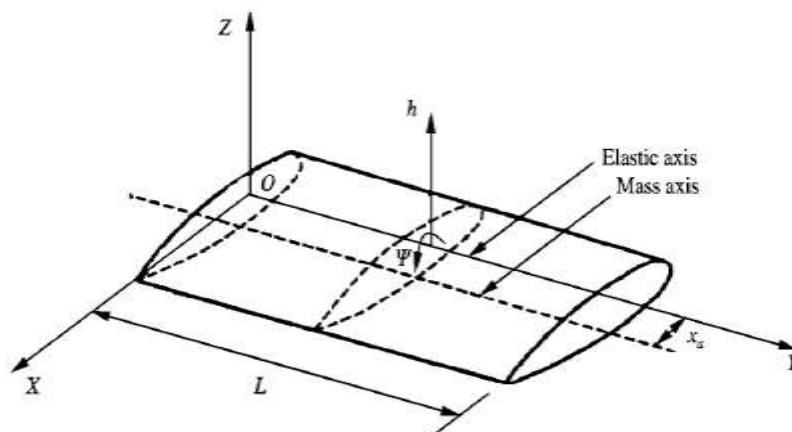

Figure 1 An aircraft wing idealised as a bending-torsion coupled beam.

In essence, the coupling between the bending and the torsional motions arises due to non-coincident mass and elastic axes which are respectively the loci of the centroid and shear centres of the beam cross-section. Thus for an aircraft wing it is not generally possible to realize a torsion-free bending displacement or a bending-free torsional rotation during its dynamic motion unless the load or the torque is applied through or about the shear centre. Given this perspective, a high aspect ratio non-uniform aircraft wing can be accordingly modelled as an assemblage of bending-torsion couple beams of the type shown in figure 1. This paper uses a dynamic stiffness approach and develops the dynamic stiffness matrix of a uniform bending-torsion coupled beam and then extends it to model a non-uniform wing.

The governing partial differential equations of motion of the bending-torsion coupled beam (wing) shown in figure 1 are given by [9, 10]

$$EIh'''' + m\ddot{h} - mx_\alpha\ddot{\psi} = 0 \tag{1}$$

$$GJ\psi'' + mx_\alpha\ddot{h} - I_\alpha\ddot{\psi} = 0 \tag{2}$$

where EI and GJ are the bending and torsional rigidities of the beam, m is the mass per unit length, I_α is the polar mass moment of inertia per length about the Y-axis and the primes and over dots denotes partial differentiation with respect to position y and time t, respectively.

For harmonic oscillation, sinusoidal variation in h and ψ with circular frequency ω may be assumed to give

$$h(y,t) = H(y)sin\omega t, \qquad \psi(y,t) = \Psi(y)sin\omega t \tag{3}$$

where $H(y)$ and $\Psi(y)$ denote the amplitude of the bending displacement and torsional rotation

Substituting equation (3) into equations (1) and (2) eliminates the time component and gives the following ordinary differential equations

$$EIH'''' - m\omega^2 H + mx_\alpha\omega^2\Psi = 0 \tag{4}$$

$$GJ\Psi'' + I_\alpha\omega^2\Psi - \omega^2 mx_\alpha H = 0 \tag{5}$$

where prime now denotes full differentiation with respect to y.

Equations (4) and (5) can be combined into a sixth order ordinary differential equation by eliminating either H or Ψ to give

$$W'''''' + \left(\frac{I_\alpha\omega^2}{GJ}\right)W'''' - \left(\frac{m\omega^2}{EI}\right)W'' - \left(\frac{m\omega^2}{EI}\right)\left(\frac{I_\alpha\omega^2}{GJ}\right)\left(\frac{I_\alpha - mx_\alpha^2}{I_\alpha}\right)W = 0 \tag{6}$$

where

$$W = H \text{ or } \Psi \tag{7}$$

Equation (6) can be non-dimensionalised by using the non-dimensionalised length ξ where

$$\xi = \frac{y}{L} \tag{8}$$

Thus, with the help of equation (8), the non-dimensional form of equation (6) becomes

$$(D^6 + aD^4 - bD^2 - abc)W = 0 \tag{9}$$

where a, b and c are non-dimensional parameters given by

$$a = \left(\frac{I_\alpha \omega^2 L^2}{GJ}\right), \qquad b = \left(\frac{m\omega^2 L^4}{EI}\right), \qquad c = \left(\frac{I_\alpha - mx_\alpha^2}{I_\alpha}\right) \qquad (10)$$

and D is the following differential operator

$$D = \frac{d}{d\xi} \qquad (11)$$

The differential equation given by equation (9) can be solved using standard procedure [9, 10] to give

$$W(\xi) = C_1 cosh\alpha\xi + C_2 sinh\alpha\xi + C_3 cos\beta\xi + C_4 sin\beta\xi + C_5 cos\gamma\xi + C_6 sin\gamma\xi \qquad (12)$$

where

$$\left. \begin{aligned}
\alpha &= \left[2\left(\frac{q}{3}\right)^{\frac{1}{2}} cos\left(\frac{\phi}{3}\right) - \frac{a}{3}\right]^{\frac{1}{2}} \\
\beta &= \left[2\left(\frac{q}{3}\right)^{\frac{1}{2}} cos\left(\frac{(\pi-\phi)}{3}\right) + \frac{a}{3}\right]^{\frac{1}{2}} \\
\gamma &= \left[2\left(\frac{q}{3}\right)^{\frac{1}{2}} cos\left(\frac{(\pi+\phi)}{3}\right) + \frac{a}{3}\right]^{\frac{1}{2}}
\end{aligned} \right\} \qquad (13)$$

with

$$q = b + \frac{a^2}{3} \qquad (14)$$

and

$$\phi = cos^{-1}\left[\frac{27abc - 9ab - 2a^3}{\left\{2(a^2 + 3b)^{\frac{3}{2}}\right\}}\right] \qquad (15)$$

In equation (12), C_1-C_6 are the integration constants resulting from the solution of the governing differential equation (9).

$W(\xi)$ of equation (12) is the solution for both the bending displacement H and the torsional rotation Ψ, but with different sets of constants. Therefore,

$$H(\xi) = A_1 cosh\alpha\xi + A_2 sinh\alpha\xi + A_3 cos\beta\xi + A_4 sin\beta\xi + A_5 cos\gamma\zeta + A_6 sin\gamma\xi \qquad (16)$$

and

$$\Psi(\xi) = B_1 cosh\alpha\xi + B_2 sinh\alpha\xi + B_3 cos\beta\xi + B_4 sin\beta\xi + B_5 cos\gamma\zeta + B_6 sin\gamma\xi \qquad (17)$$

The two different sets of constants $A_1 - A_6$ and $B_1 - B_6$ in equations (16) and (17) can be related with the help of either equation (4) or equation (5) to give.

$$\left. \begin{aligned}
B_1 &= k_\alpha A_1, & B_3 &= k_\beta A_3, & B_5 &= k_\gamma A_5 \\
B_2 &= k_\alpha A_2, & B_4 &= k_\beta A_4 & B_6 &= k_\gamma A_6
\end{aligned} \right\} \qquad (18)$$

where

$$k_\alpha = \frac{b - \alpha^4}{bx_\alpha}, \quad k_\beta = \frac{b - \beta^4}{bx_\alpha}, \quad k_\gamma = \frac{b - \gamma^4}{bx_\alpha} \qquad (19)$$

The expressions for bending rotation $\theta(\xi)$, bending moment $M(\xi)$, shear force $S(\xi)$ and torque $T(\xi)$ are given by

$$\theta(\xi) = H'\left(\frac{\xi}{L}\right) = \left(\frac{1}{L}\right)\{A_1\alpha sinh\alpha\xi + A_2\alpha cosh\alpha\xi - A_3\beta sin\beta\xi + A_4\beta cos\beta\xi$$
$$-A_5\gamma sin\gamma\xi + A_6\gamma cos\gamma\xi\} \qquad (20)$$

$$M(\xi) = -\left(\frac{EI}{L^2}\right)H''(\xi) = -\left(\frac{EI}{L^2}\right)\{A_1\alpha^2 cosh\alpha\xi + A_2\alpha^2 sinh\alpha\xi - A_3\beta^2 cos\beta\xi - A_4\beta^2 sin\beta\xi -$$
$$A_5\gamma^2 cos\gamma\xi - A_6\gamma^2 sin\gamma\xi\} \qquad (21)$$

$$S(\xi) = \left(\frac{EI}{L^3}\right)\{A_1\alpha^3 sinh\alpha\xi + A_2\alpha^3 cosh\alpha\xi + A_3\beta^3 sin\beta\xi - A_4\beta^3 cos\beta\xi + A_5\gamma^3 sin\gamma\xi -$$
$$A_6\gamma^3 cos\gamma\xi\} \qquad (22)$$

$$T(\xi) = \left(\frac{GJ}{L}\right)\Psi'(\xi) = \left(\frac{GJ}{L}\right)\{B_1\alpha sinh\alpha\xi + B_2\alpha cosh\alpha\xi - B_3\beta sin\beta\xi + B_4\beta cos\beta\xi - B_5\gamma sin\gamma\xi +$$
$$B_6\gamma cos\gamma\xi\} \qquad (23)$$

With the help of equations (16)-(23), the dynamic stiffness matrix of the coupled bending-torsion beam element which is essentially an aircraft wing element can be developed by applying the boundary conditions for displacements and forces at the ends of the elements.

Referring to figure 2, the boundary conditions for displacements are

$$\left.\begin{array}{lll}\text{At } y = 0 \ (\xi=0): \ H = H_1, & \theta = \theta_1 & \Psi = \Psi_1 \\[2mm] \text{At } y = L \ (\xi = 1): H = H_2, & \theta = \theta_2 & \Psi = \Psi_2\end{array}\right\} \qquad (24)$$

Similarly, referring to figure 3, the boundary conditions for the forces are

$$\left.\begin{array}{lll}\text{At } y = 0 \ (\xi=0): S = S_1, \ \ M = M_1 & T = -T_1 \\[2mm] \text{At } y = L \ (\xi = 1): S = -S_2, M = -M_2 & T = T_2\end{array}\right\} \qquad (25)$$
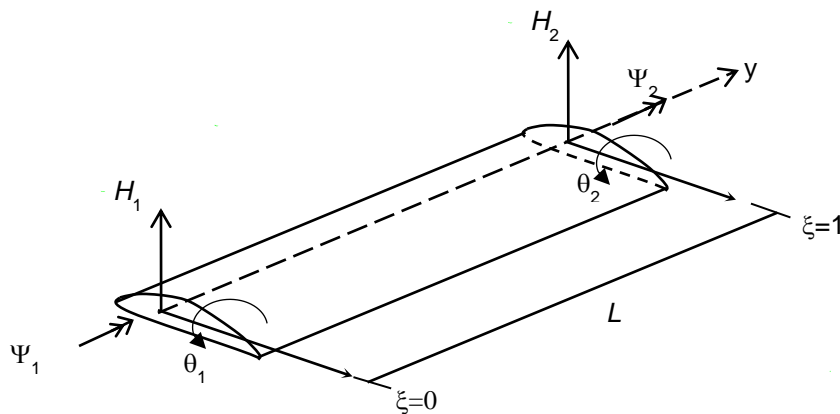

Figure 2. Boundary conditions for displacements of an aircraft wing element.
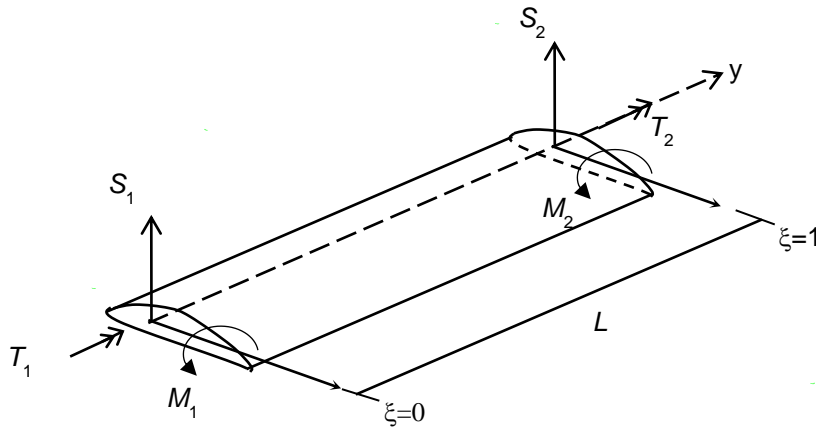
Figure 3. Boundary conditions for forces of an aircraft wing element.

Substituting the boundary conditions for displacements given by equation (24) into equations (16), (20) and (17), one obtains the following matrix relationship

$$
\begin{bmatrix} H_1 \\ \theta_1 \\ \Psi_1 \\ H_2 \\ \theta_2 \\ \Psi_2 \end{bmatrix} = \begin{bmatrix} 1 & 0 & 1 & 0 & 1 & 0 \\ 0 & \alpha/L & 0 & \beta/L & 0 & \gamma/L \\ k_\alpha & 0 & k_\beta & 0 & k_\gamma & 0 \\ C_{h_\alpha} & S_{h_\alpha} & C_\beta & S_\beta & C_\gamma & S_\gamma \\ \alpha S_{h_\alpha}/L & \alpha C_{h_\alpha}/L & -\beta S_\beta/L & \beta C_\beta/L & -\gamma S_\gamma/L & \gamma C_\gamma/L \\ k_\alpha C_{h_\alpha} & k_\alpha S_{h_\alpha} & k_\beta C_\beta & k_\beta S_\beta & k_\gamma C_\gamma & k_\gamma S_\gamma \end{bmatrix} \begin{bmatrix} A_1 \\ A_2 \\ A_3 \\ A_4 \\ A_5 \\ A_6 \end{bmatrix}
\tag{26}
$$

or

$$
\Delta = \mathbf{BA}
\tag{27}
$$

where $\mathbf{A}$ is the contact vector comprising the constants A_1 - A_6 and

$$
C_{h_\alpha} = \cosh\alpha; \; S_{h_\alpha} = \sinh\alpha; \; C_\beta = \cos\beta; \; S_\beta = \sin\beta; \; C_\gamma = \cos\gamma; \; S_\gamma = \sin\gamma
\tag{28}
$$

Substituting the boundary conditions for forces given by equation (25) into equations (22), (21) and (23), one obtains the following matrix relationship

$$
\begin{bmatrix} S_1 \\ M_1 \\ T_1 \\ S_2 \\ M_2 \\ T_2 \end{bmatrix} = \begin{bmatrix} 0 & W_3\alpha^3 & 0 & -W_3\beta^3 & 0 & -W_3\gamma^3 \\ -W_2\alpha^2 & 0 & W_2\beta^2 & 0 & W_2\gamma^2 & 0 \\ 0 & -W_1k_\alpha\alpha & 0 & -W_1k_\beta\beta & 0 & -W_1k_\gamma\gamma \\ -W_3\alpha^3 S_{h_\alpha} & -W_3\alpha^3 C_{h_\alpha} & W_3\beta^3 S_\beta & W_3\beta^3 C_\beta & -W_3\gamma^3 S_\gamma & W_3\gamma^3 C_\gamma \\ W_2\alpha^2 C_{h_\alpha} & W_2\alpha^2 S_{h_\alpha} & -W_2\beta^2 C_\beta & -W_2\beta^2 S_\beta & -W_2\gamma^2 C_\gamma & -W_2\gamma^2 S_\gamma \\ W_1k_\alpha\alpha S_{h_\alpha} & W_1k_\alpha\alpha C_{h_\alpha} & -W_1k_\beta\beta S_\beta & W_1k_\beta\beta C_\beta & -W_1k_\gamma\gamma S_\gamma & W_1k_\gamma\gamma C_\gamma \end{bmatrix} \begin{bmatrix} A_1 \\ A_2 \\ A_3 \\ A_4 \\ A_5 \\ A_6 \end{bmatrix}
\tag{29}
$$

or

$$\mathbf{F} = \mathbf{D}\mathbf{A} \tag{30}$$

where

$$W_1 = \frac{GJ}{L}; \ \ W_2 = \frac{EI}{L^2}; \ \ W_3 = \frac{EI}{L^3} \tag{31}$$

The constant vector **A** can now be eliminated from equations (27) and (30) to give the following force-displacement relationship

$$\mathbf{F} = \mathbf{K}\,\Delta \tag{32}$$

where **K** is the 6×6 frequency dependent dynamic stiffness matrix given by

$$\mathbf{K} = \mathbf{D}\,\mathbf{B}^{-1} \tag{33}$$

The dynamic stiffness matrix of equation (33) representing a bending-torsion coupled beam such as an aircraft wing can now be used to model an aircraft wing. A non-uniform aircraft wing can be modelled as an assembly of many uniform dynamic stiffness elements. For instance, the unswept cantilever wing of figure 4 can be modelled as a stepped cantilever beam (wing) as shown in figure 5 where the non-uniform wing is split into 10 uniform dynamic stiffness elements. The dynamic stiffness elements of each of the 10 elements can be assembled to form the overall dynamic stiffness matrix of the complete wing. The straight unsweep wing and its idealisation in figures 4 and 5 are shown only for convenience, but the theory given above is sufficiently general and can handle swept and other wings with complex geometries.

The solution procedure to extract the natural frequencies and mode shapes from the overall dynamic stiffness matrix of the wing is based on the application of the Wittrick-Williams algorithm [8] which has featured in hundreds of papers. The algorithm is particularly suitable in solving free vibration problem using the dynamic stiffness method. The working principle of the algorithm is briefly summarised in the next section.
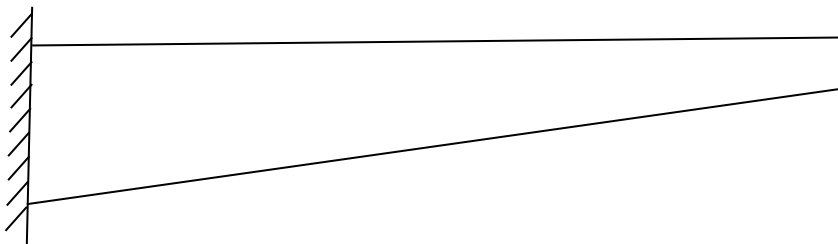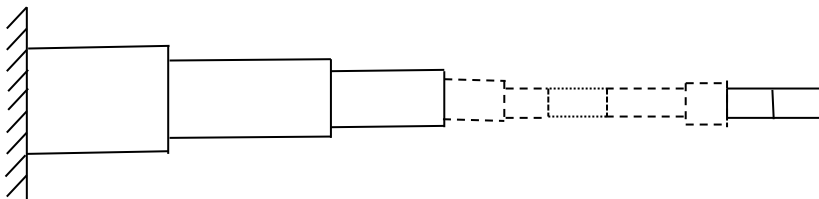

Figure 4. A non-uniform cantilever wing.

Figure 5. A non-uniform cantilever wing idealised as a stepped beam.

2.2 Application of the Wittrick-Willams algorithm

The dynamic stiffness matrix of equation (33) can now be used to compute the natural frequencies and mode shapes of aircraft wings. A non-uniform and/or swept wing can be analysed for its natural frequencies and mode shapes by idealising it as an assemblage of many uniform dynamic stiffness elements of bending-torsion coupled beams. The natural frequency calculation is accomplished by applying the Wittrick-Williams algorithm [8] which has received extensive coverage in the literature. Before applying the algorithm the dynamic stiffness matrices of all individual elements (see figures 4 and 5) need to be assembled to form the overall dynamic stiffness matrix $\mathbf{K}_f$ of the complete wing. The algorithm monitors the Sturm sequence condition of $\mathbf{K}_f$ in such a way that there is no possibility of missing any natural frequency of the wing. The application procedure of the algorithm is briefly summarised as follows.

Suppose that ω denotes the circular (or angular) frequency of the vibrating wing. Then according to the Wittrick-Williams algorithm [8], j, the number of natural frequencies passed, as ω is increased from zero to ω^*, is given by

$$j = j_0 + s\{\mathbf{K}_f\} \tag{34}$$

where $\mathbf{K}_f$, the overall dynamic stiffness matrix of the wing whose elements depend on ω is evaluated at $\omega = \omega^*$; $s\{\mathbf{K}_f\}$ is the number of negative elements on the leading diagonal of $\mathbf{K}_f^\Delta$, $\mathbf{K}_f^\Delta$ is the upper triangular matrix obtained by applying the usual form of Gauss elimination to $\mathbf{K}_f$, and j_0 is the number of natural frequencies of the wing still lying between $\omega = 0$ and $\omega = \omega^*$ when the displacement components to which $\mathbf{K}_f$ corresponds are all zeros. (Note that the structure can still have natural frequencies when all its nodes are clamped, because exact member equations allow each individual member to displace between nodes with an infinite number of degrees of freedom, and hence infinite number of natural frequencies between nodes.) Thus

$$j_0 = \sum j_m \tag{35}$$

where j_m is the number of natural frequencies between $\omega = 0$ and $\omega = \omega^*$ for an individual component member with its ends fully clamped, while the summation extends over all members of the structure. Thus, with the knowledge of equations (34) and (35), it is possible to ascertain how many natural frequencies of the wing lie below an arbitrarily chosen trial frequency (ω^*). This simple feature of the algorithm can be used to converge upon any required natural frequency to any desired accuracy. As successive trial frequencies can be chosen, computer implementation of the algorithm is very simple. However, for a detailed understanding, readers are referred to the original work of Wittrick and Williams [8].

3. Results and discussion

Using the above theory, two categories of aircraft wings with cantilever boundary condition at the root are analysed for their modal characteristics. In the first category, a class of high aspect ratio, high performance sailplane wings are considered. A typical layout of such a sailplane is shown in figure 6. Results for natural frequencies and mode shapes are computed for two sailplanes (S1 and S2) with spans 22m and 15m, respectively. Some particulars of the two sailplanes are given in Table 1. The second category of aircraft wings analysed belongs to transport airliners. A typical layout is shown in figure 7. Four wings of transport airliners (T1, T2, T3 and T4) with particulars given in Table 2 are analysed. In all cases, 10 dynamic stiffness elements were used to represent each wing. The data used for the stiffness (*EI* and *GJ*) and mass/inertia (*m* and I_α) properties of the wings and the shear centre locations (x_α) were calculated from the cross-sectional drawings of the wings expending considerable efforts. These data for the six aircraft are far too extensive to report in this paper.
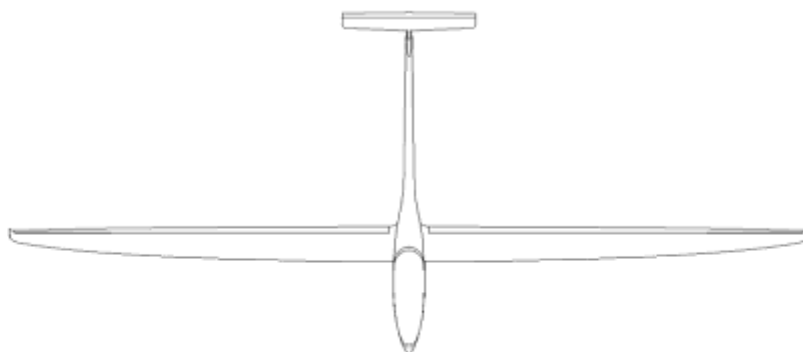
Figure 6. A general lay-out of a typical sailplane.

Figure 7. A general lay-out of a typical transport aircraft.

Table 1. Particulars of sailplanes

Parameters	Sailplane	
	Sailplane-S1	Sailplane-S2
Wing Span (m)	22	15
Wing Area (m^2)	15.44	10.05
Aspect Ratio	31.35	22.4
Wing Root Chord (m)	1.0	0.9
Wing Tip Chord (m)	0.4	0.4
Sweep angle (deg)	0	0
Length overall (m)	7.6	6.72
Height Overall (m)	2.0	2.0
Weight Empty (kg)	390	234
Max Take-off weight (kg)	550	440
Max Wing Loading (kg/m^2)	37	36
Max Cruising Speed (knots)	135	105

Table 2. Particulars of transport airliners.

Parameters	Transport airliner			
	T1	T2	T3	T4
Wing Span (m)	40	30	35	60
Wing Area (m^2)	162	93	123	362
Aspect Ratio	10	9	10	10
Wing Root Chord (m)	5.0	5.5	6.0	10.5
Wing Tip Chord (m)	2.5	1.5	1.5	2.5
Sweep angle (deg)	0	28	28	28
Length overall (m)	30	36	38	60
Height Overall (m)	12	11	12	17
Weight Empty (kg)	34,000	26,000	42,000	130,000
Max Take-off weight (kg)	70,000	46,000	74,000	275,000
Max Wing Loading (kg/m^2)	434	511	600	760
Max Cruising Speed (knots)	348	529	516	569
Range (nmi)	2835	2400	2592	8000

The first five natural frequencies of the six aircraft wings (two for sailplanes and four for transport airliners) are shown in Table 3. The letters B and T shown in the parenthesis indicate bending and torsion dominated modes, respectively whereas the letter C indicates a coupled mode with substantial amount of both bending and torsional displacements. It should be noted that sailplane wings do not carry engines whereas the transport airline wings have engine(s) with mass and inertia properties which have significant effects on natural frequencies. (Engine mass is a huge proportion of the total wing mass.) The mode shapes for the two sailplanes corresponding to the natural frequencies of Table 3 are shown in figure 8 whereas those of the four transport airliner wings are shown in figures 9 and 10, respectively.

Table 3. Natural frequencies of sailplane and transport airliner wings. (B): Bending dominated mode; (T): Torsional dominated mode;(C): Bending-Torsion coupled mode.

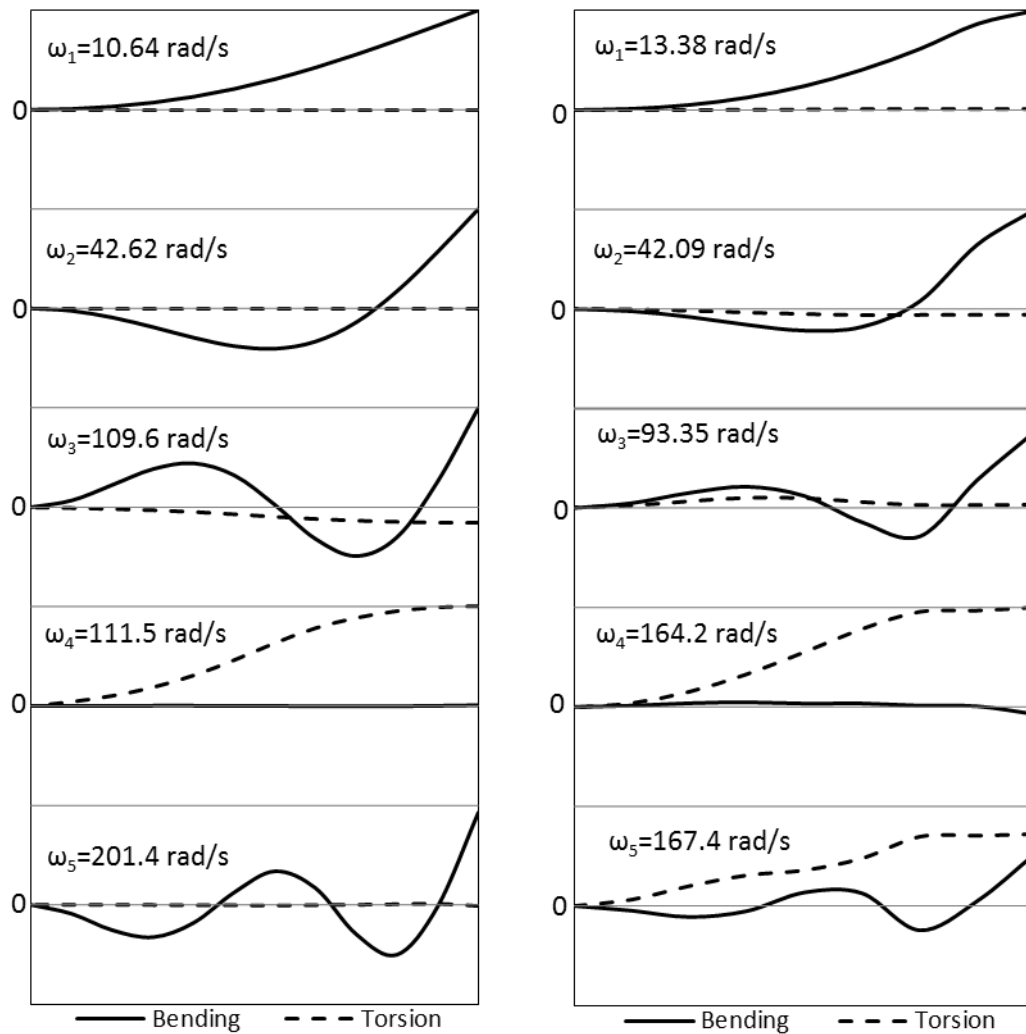| Aircraft Category	Natural Frequencies (ω_i) (rad/s)				
	ω_1	ω_2	ω_3	ω_4	ω_5
Sailplane S1	10.64(B)	42.62(B)	109.6(B)	111.5(T)	201.4(B)
Sailplane S2	13.38(B)	42.09(B)	93.35(B)	164.2(T)	167.4(C)
Transport Airliner T1	11.52(B)	33.09(B)	45.43(C)	87.85(B)	97.76(C)
Transport Airliner T2	19.71(B)	55.29(B)	100.2(B)	120.9(C)	197.7(C)
Transport Airliner T3	11.99(B)	34.69(B)	67.66(B)	74.14(T)	118.4(C)
Transport Airliner T4	8.994(B)	26.45(B)	47.64(T)	72.70(B)	94.64(T)

Figure 8. Natural frequencies and mode shapes of Sailplane wings S1 and S2.

Clearly, the first three modes of the cantilever wings of the two sailplanes S1 and S2 are bending modes whereas the fourth mode for each of them is a pure torsional mode, see figure 8. The fifth mode for the S1 wing is a bending mode. By contrast, for the S2 wing it is a coupled mode.
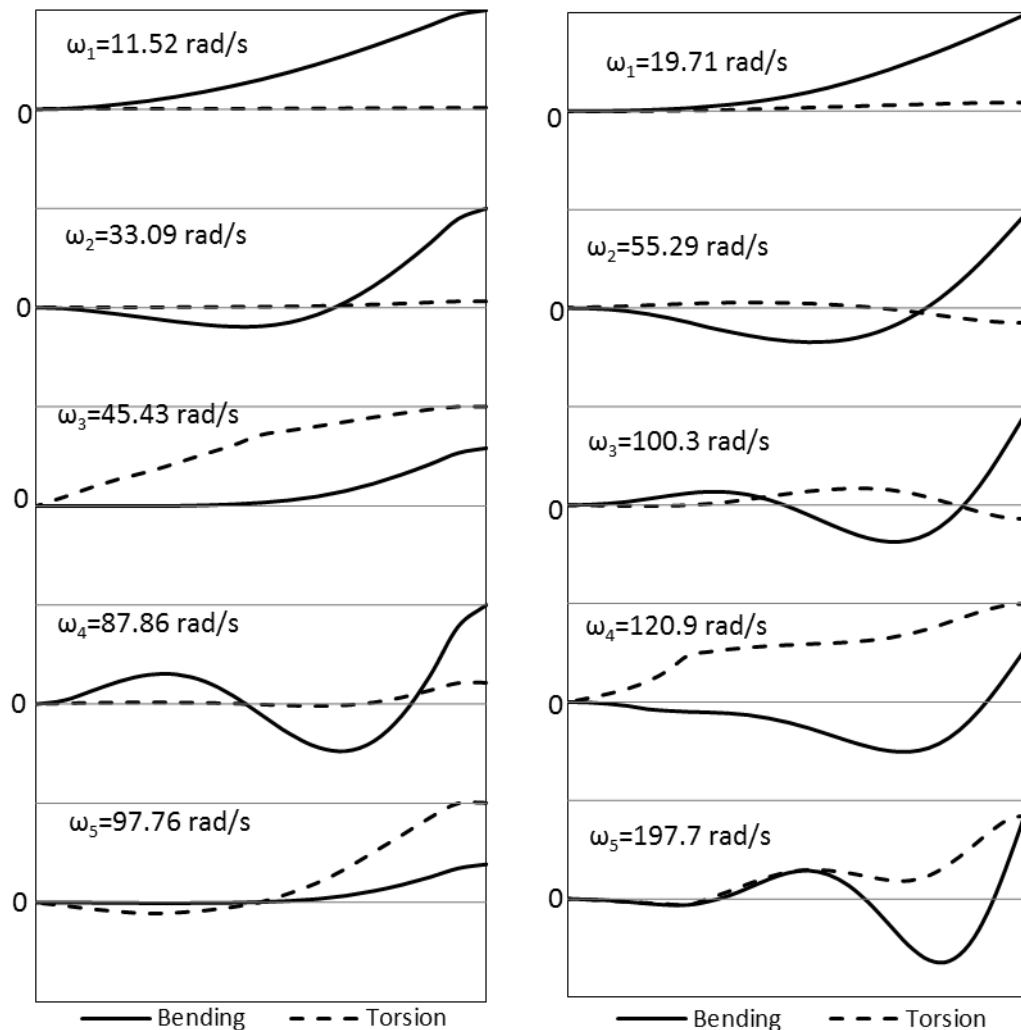
Figure 9. Natural frequencies and mode shapes of transport airliner wings T1 and T2.

Referring to Table 3 and figure 9, the first two modes of the cantilever wings of transport airliner T1 and T2 are essentially bending modes, but the nature of the third mode for the two wings differs quite significantly. For T1, it is basically a coupled mode dominated by torsional displacement, but for T2, it is a bending dominated mode. The fourth mode for T1 is bending dominated, but for T2 it is actually a bending-torsion coupled mode. To all intents and purposes, the fifth mode for both T1 and T2 is a coupled mode. Now referring to figure 10, the mode shapes for T3 and T4 wings are discussed. The first two modes for these two cantilever wings are essentially bending modes as was the case with T1 and T2 wings. However, the third mode for T3 and T4 are different. For the T3 wing, it is a bending-torsion coupled mode, but dominated by bending whereas for the T4 wing, it is a pure torsional mode. The fourth mode for the T3 wing is mainly a torsion dominated mode with some bending deformation present, but for the T4 wing it is a bending dominated mode with a small amount of torsion present. The fifth mode for T3 is a coupled mode whereas for T4, it is a torsional mode.
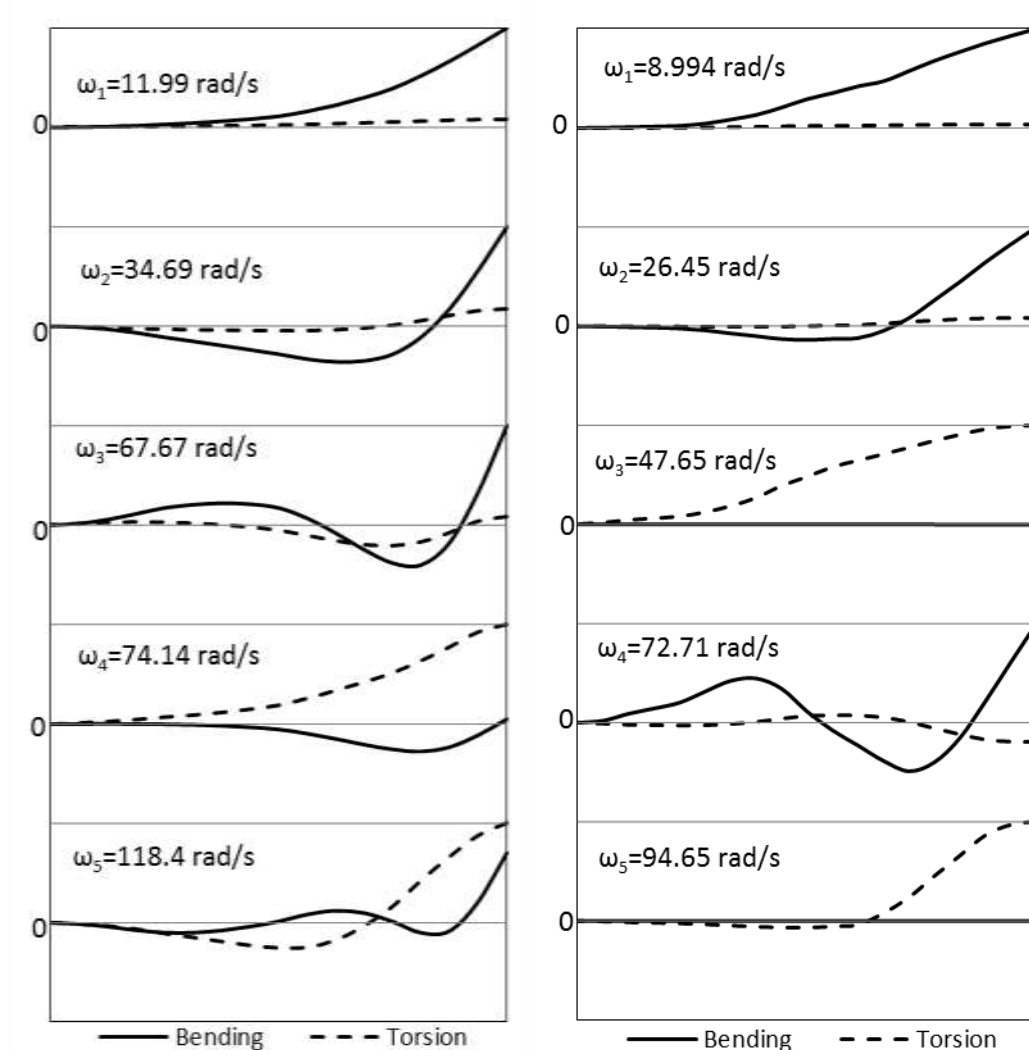
Figure 10. Natural frequencies and mode shapes of transport airliner wings T3 and T4.

4. Conclusions

Using the dynamic stiffness method and by applying the Wittrick-Williams algorithm, the modal behaviour of two sailplane and four transport aircraft wings is investigated. Natural frequencies and mode shapes for these wide ranging aircraft wings for cantilever boundary conditions are illustrated. The results are examined and discussed. In general, the first two modes for each of the six aircraft are effectively bending modes, but the third mode is either bending or torsional or a coupled mode depending on the type of the wing analysed. The fourth mode is again either torsion or bending dominated or even coupled. The same observation is made for the fifth mode. The investigation paves the way to establish trends for the modal behaviour of high aspect ratio aircraft wings.

Acknowledgements

5. References

[1]   Banerjee J R 1984 Flutter characteristics of high aspect ratio tailless aircraft *J. Aircraft* **21** 733-735.

[2]   Banerjee J R 1988 Flutter modes of high aspect ratio tailless aircraft *J. Aircraft* **25** 473-476.

[3]   van Schoor M C and von Flotow A H 1990 Aeroelastic characteristics of highly flexible aircraft, *J Aircraft* **27** 901-908.

[4]   Eslimy-Isfahany S H R, Banerjee J R and Sobey A J 1996 Response of a bending-torsion coupled beam to deterministic and random loads *J. Sound Vib*. **195** 267-283.

[5]   Banerjee J R, Patel M H, Done G T S, Butler R and Lillico M 1998 Free vibration and flutter sensitivity analyses of a large transport aircraft *Proc. 7th AIAA/USAF/NASA/ISSMO Sympos. on Multidisc. Analys. and Optimis,* St. Louis, Missouri, USA, Paper No. 98-4765.

[6]   Tang D and Dowell E H 2001 Experimental and theoretical study on aeroelastic response of high aspect ratio wings, *AIAA* **39** 1430-1441.

[7]   Banerjee J R, Liu X and Kassem H I 2014 Aeroelastic stability of high aspect ratio aircraft wings *J. Appl. Nonlin. Dyn.* **3** 413-422.

[8]   Wittrick W H and Williams F W 1971 A general algorithm for computing natural frequencies of elastic structures *Quart. J. Mech. and Appl. Math.* **24** 263-284.

[9]   Banerjee J R 1989 Coupled bending-torsional dynamic stiffness matrix for beam elements *Int. J. Num. Meth. Eng.* **28** 1283-1298.

[10]   Banerjee J R 1991 A FORTRAN program for computation of coupled bending-torsional dynamic stiffness matrix of beam elements *Adv. Eng. Software*, **13** 17-24.